Carbon 130 (2018) 614–622

Contents lists available at ScienceDirect

Carbon

journal homepage: www.elsevier.com/locate/carbon

Non-linear thermogravimetric mass spectrometry of carbon materials providing direct speciation separation of oxygen functional groups

Pascal Düngen [a], Robert Schlögl [a, b], Saskia Heumann [a, *]

[a] Max-Planck-Institut für Chemische Energiekonversion, Stiftstraße 34-36, 45470 Mülheim an der Ruhr, Germany
[b] Fritz-Haber-Institut der Max-Planck-Gesellschaft, Faradayweg 4-6, 14195 Berlin, Germany

ARTICLE INFO

Article history:
Received 11 December 2017
Received in revised form
10 January 2018
Accepted 11 January 2018

Keywords:
Multi-walled carbon nanotubes
Thermal decomposition
Oxygen functional groups
Atomic layer deposition
Selective reactivity

ABSTRACT

Thermogravimetric mass spectrometry (TG-MS) is an established way to analyze oxygen containing surface functional groups of carbon materials. Thermal stabilities and structures of functional groups influence their decomposition temperatures and products (CO, CO_2). In this work, a non-linear procedure with isothermal steps is presented enabling a separation of functional groups by different decomposition temperatures. Nitrosulfuric acid functionalized carbon materials like multi-walled carbon nanotubes (MWCNT) and graphite were used to design the temperature program. Comparative studies of linear and non-linear heating experiments in argon and hydrogen containing atmosphere were performed to state the benefits and limits of both methods. The distinct advantage of non-linear thermal analysis is demonstrated by an application-oriented experiment where only selected functional groups are consumed.

1. Introduction

Multi-walled carbon nanotubes (MWCNT) are highly desired materials for numerous applications. Due to their unique structure they combine graphitic properties like high conductivity, thermal and mechanical stability with high surface area (250 m^2/g) [1–4]. Properties of the MWCNT are strongly linked to the amount and kind of functional groups on the surface [5–7]. With an increasing amount of functional groups the conductivity and stability of MWCNT will unavoidably change. In catalysis, MWCNT are often used as support materials for small active particles [1,8]. The functional groups on the surface of the supporting MWCNT can influence the stability of the compound material. Hence, particle attachment and solubility will be influenced by the surface properties. In some cases functional groups show catalytic activities by themselves [9,10]. To describe the interaction between metal catalysts and functional groups, or to determine the catalytic activity of the carbon material itself, it is necessary to qualitatively and quantitatively identify functional groups and describe the changes to such groups before and after their use in a catalytic reaction [11,12]. Post-analysis therefore allows one to monitor the chemical changes, and to identify functional groups that are consumed or produced during a reaction. Several approaches are used to overcome this challenge. For instance titration methods use the different pk_a values of functional groups for the quantification. The conversion of functional groups, diffusion and acid residuals of MWCNT pre-treatments often impede a former characterization of functional groups [13]. Catalytic tests like the oxidation of isopropanol are used to generate sum parameter where acidic and alkaline functional groups are separated. However, the reaction temperature applied during this catalytic test already changes the composition of functional groups and influences the quantification [14].

Thermogravimetric mass spectrometry is a common way to analyze surface functional groups on carbon materials [15,16]. During the thermal treatment, oxygen-containing functional groups, depending on their structure, decompose into CO_2 or CO. Traditionally, TPD approaches use solely heating rates in argon atmosphere with a linear temperature program. Results gained out of these experiments do not enable the exact determination of the decomposition temperature of different functional groups. Overlapping signals due to the decomposition of multiple functional groups with similar decomposition temperatures hinders an exact determination of decomposition temperature [17–20]. Recently, thermal stabilities of different surface functional groups were determined by a combination of temperature programmed

* Corresponding author.
E-mail address: saskia.heumann@cec.mpg.de (S. Heumann).

https://doi.org/10.1016/j.carbon.2018.01.047

desorption (TPD), X-ray Photoelectron Spectroscopy (XPS), titration, and catalytic test reaction experiments [21]. Due to the combination of these methods an exact determination and assignment of the decomposition temperatures of functional groups, where maxima of the decomposition products are analyzed, was possible (see Table 1). Even if the decomposition temperatures of the functional groups have already been discussed the problem of overlapping signals during TPD measurements still exists, and prohibits differentiation of functional groups. For a quantitative analysis of functional groups via TPD, a separation during the decomposition process is required.

The present work focuses on separating the decomposition products of functional groups during TPD measurements based on the observations summarized in Table 1. To accomplish this, we used a non-linear temperature program procedure. This method is now referred to as an isothermal temperature program. Due to the insertion of isothermal steps during the heating process, the overlay between different desorption process from chemically different functional groups can be avoided by completing each desorption process prior to increasing the decomposition temperature. . The temperatures of these isothermal steps were determined by analyzing the peak shape of the individual ion currents. Moreover, literature values were used to confirm the temperatures determined for the separation of functional groups [19–26]. Applying an isothermal temperature program during the TPD analysis of carbon materials affords the following benefits:

- Isolation of different functional groups due to thermal separation
- Identification of decomposition temperature ranges for different functional groups
- Particular detection of decomposing products of functional groups with different decomposition temperatures
- Detection of interconversion of functional groups before and after reaction conditions (e.g. consumption, formation, conversion etc.)

In addition to the influence of isothermal steps on the detected signals of decomposition products, the influence of different heating rates on the decomposition was investigated. Thereby, the influence of kinetic hindrances on the CO_2^+ and CO^+ ion currents was investigated. The shapes of the ion currents were not affected by the heating rate and shoulders appearing during the analysis are related to different functional groups.

2. Materials and methods

2.1. Functionalization of carbon materials

Graphite (Merck Millipore) as well as MWCNT produced from Shangdong Dazhang Nano Materials Co. were treated with nitro-sulfuric acid (vol% ratio: 1:1; nitric acid 65%: sulfuric acid 98%) to create oxygen containing functional groups on the surface of the MWCNT. The procedure of functionalization is described in detail elsewhere [27]. Briefly 10 g of carbon material was mixed with 500 ml of acid. The mixture was heated to 105 °C and stirred for 4 h. Afterward, the modified carbon materials were filtered and residuals of acid were washed out over several hours in a washing cell. The oxidized carbon was dried in a vacuum-oven at 80 °C for 12 h. To test the applicability of the developed temperature program two commercially available graphitic reference materials, active char and Vulcan XC 75R, were also analyzed. These materials were not pre-treated before analysis.

Table 1
Overview of decomposition temperatures of functional groups in carbon structures from Ref. [21].

Functional group	Temperature [°C]	Detected species
Carboxyl	275	$CO_2 + H_2O$
Anhydride	435, 460	$CO_2 + CO$
Lactone	650	CO_2
Phenol	735	CO
Ether	735	CO
Carbonyl/ Quinone	920	CO

2.2. Thermal analysis procedure

Thermal analysis was performed using a STA 449 F3 Jupiter® QMS4 setup from Netzsch with an argon gas flow of 70 ml/min. Isothermal steps were inserted during thermogravimetric mass spectrometry (TG-MS) analysis to separate functional groups with different decomposition temperatures. The optimum temperature of the implemented isothermal step was judged by the peak shapes of both CO^+ and CO_2^+ signals. Heating rates were varied between 10 K/min and 50 K/min. Based on the investigated results a heating rate of 20 K/min was applied in-between the isothermal steps to avoid overheating while maintaining satisfactory signal intensities, whereas a heating rate of 50 K/min was chosen after the last isothermal step, due to higher signal intensities. Reproducibility was confirmed by three iterations.

2.3. Atomic layer deposition

A commercial atomic layer deposition (ALD) setup (Savannah S200, Ultratech) was used to deposit vanadium oxide on the functionalized MWCNT. Vanadium(V) triisopropoxide (CAS: 5588-84-1, Sigma-aldrich) precursor was heated to 70 °C and exposed for 0.5 s to the acid pre-treated MWCNT. This procedure was repeated for 250 cycles, respectively. Organic residuals of the precursor were purged after each cycle using water pulses of 0.5 s. The temperature of the reaction chamber during the process was held constant at 150 °C.

3. Results and discussion

3.1. Determination of isothermal steps

Thermal decomposition of oxidized carbon materials combined with simultaneous detection of released gaseous products enables the determination of different thermal stabilities of functional groups. To ensure a reliable analysis, the decomposition of surface functional groups at different temperatures needs to be independent of gas transport effects. Therefore, comparison of MWCNT, as representative of high surface materials with a surface area of 239 m^2/g and a mesoporous character was compared with graphite, as nonporous material with a surface area of 20 m^2/g. Non-porous MWCNT forms bundles due to agglomeration, corresponding empty spaces between MWCNT provides a mesoporous character of these samples [28]. Specific surface areas were determined by N_2 sorption experiments and analyzed by Brunauer-Emmet-Teller (BET) theory showing type II hysteresis for graphite and type IV for MWCNT (supporting information S1). Hence, both materials show similar behavior of relatively weak adsorbent-adsorbate interactions with molecular clustering at higher p/p^0, and subsequent pore filling in the case of MWCNT.

Different heating rates during the thermal analysis were applied to investigate how heating width affects peak width, position and intensity of the detected CO_2^+ and CO^+ signals of the two

representative carbon materials (Fig. 1.) as well as the influence on the detected ratio of these molecular fragments, as shown in supporting information Fig. 2. The comparison of MWCNT and graphite CO_2^+ and CO^+ MS ion currents (Fig. 1) reveals clear differences in intensity and peak width, whereas the peak positions of MWCNT and graphite are similar. In general, the peak maxima are slightly shifted to higher temperatures with increasing heating rates caused by the accruing thermal gradient within the samples [29]. This effect is most apparent in the case of MWCNT.

Differences in ion currents are only minor, indicating that the decomposition temperatures of the functional groups for both materials are similar. The porous character of MWCNT affects only the diffusion of the released gases and results in a peak broadening. Additionally, Fig. 1 reveals that the peak shape of the ion currents becomes more pronounced with increasing heating rates.

The total amount of released CO_2 and CO dependents from the heating rate (supporting information Fig. 2). At the same time, the ratio of the two detected gases changes. With increasing heating rate, the total amount of detected CO_2 decreases, whereas the amount of detected CO increases as a result of secondary reactions. This phenomenon was already discussed in the literature for activated carbons [30]. Desorbed CO reacts with remaining functional groups and defects in the carbon structure, resulting in the formation of CO_2 (Eq (1)).

$$CO + C(O) \rightleftarrows C_f + CO_2 \quad \Delta G^0 = -71\ kJ/mol \tag{1}$$

The exoergic reaction is thermodynamically hindered at higher heating rates, resulting in ostensibly lower CO at lower heating rates. Therefore, the secondary reaction complicates a quantitative analysis of functional groups based on thermal decomposition products. By gas flow variations of the carrier gas the influence of reaction 1on the TPD analysis can be quantitative investigated. In case of significant influences of reaction 1, the applied method of separation allows only a semi-quantitative determination of functional group amount.

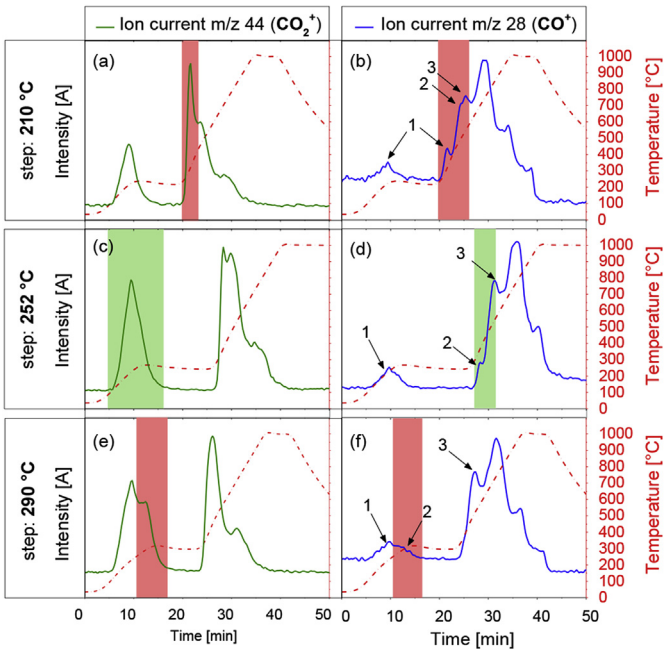

Fig. 2. Example for the implementation of isothermal steps to separate the carboxylic group. The ion current of *m*/*z* 44 (left) and *m*/*z* 28 (right) of three independent TPD experiments with isothermal steps at (a/b) 210 °C (c/d) 252 °C and (e/f) 290 °C are illustrated. The temperature profile is shown by the dashed red line. The arrows label the CO^+ signals of the first three functional groups with increasing thermal stability accordingly to the numbers in Fig. 3c. (A colour version of this figure can be viewed online.)

A heating rate of 20 K/min was chosen as an optimal compromise in comparison to higher heating rates to suppress secondary reactions. Furthermore, this heating rate generates well defined ion current profiles, and ensures less overheating at each isothermal

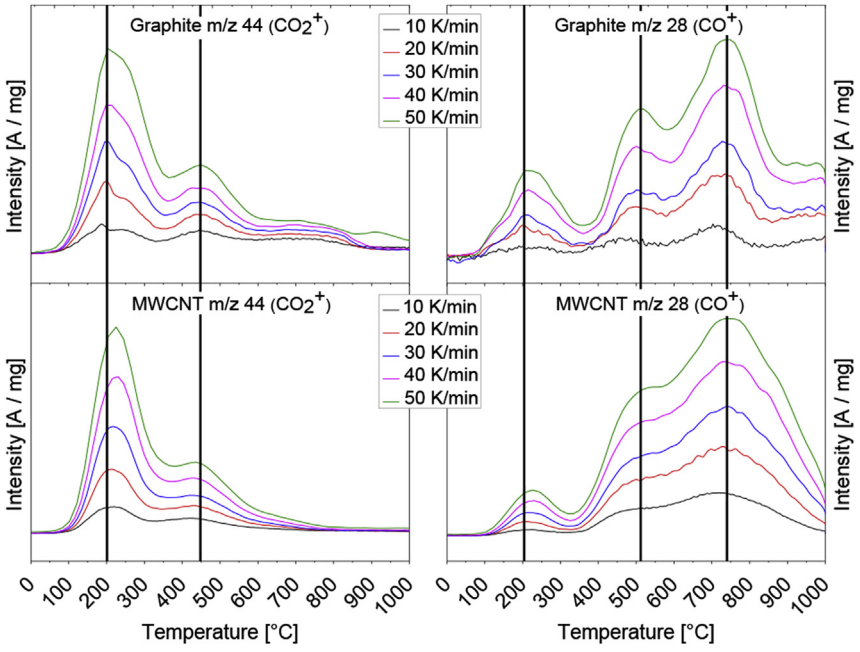

Fig. 1. Ion currents of CO_2^+ (*m*/*z* 44) and CO^+ (*m*/*z* 28) determined with different linear heating rates of graphite (top) and MWCNT (down). Vertical lines assist for better comparison. (A colour version of this figure can be viewed online.)

step. In accordance to the presence of six types of oxygen functional groups with different decomposition temperatures in the carbon structure (Table 1), six isothermal steps had to be implemented and optimized. All determined decomposition temperatures correspond to the complete decomposition process of each functional group rather than the onset of the decomposition. The separation of different functional groups with isothermal steps during the TPD analysis is based on the theory that functional groups of certain kinds decompose at defined temperatures, whereas functional groups with higher thermal stability are not affected.

The general procedure for the separation will be explained in detail for the carboxylic groups, exhibiting the lowest thermal stability. TG-MS profiles for group separation of additional functionalities are available in the supporting information (S3-6). Fig. 2 shows the ion current profiles of CO_2^+ (left row) and CO (right row) with three different isothermal steps. The middle panel (Fig. 2c/d) shows the ion current profiles of the accurately determined decomposition temperature of the carboxylic group at 252 °C, which is also in agreement with literature values [19,21]. Exemplary, MS profiles with inserted steps at 210 °C (Fig. 2 a/b) and 290 °C (Fig. 2 e/f) of too-low and too-high decomposition temperatures are shown, respectively. The heating rates up to the first isothermal step were 20 K/min, as described earlier. After the isothermal steps, the heating rates were increased to 50 K/min to obtain a more pronounced peak shape.

The determination of the isothermal steps was validated by the peak shapes of the CO_2 and CO MS signals. The main decomposition product of carboxylic groups, is CO_2. Nevertheless, fragmentation in the mass spectrometer results in a corresponding CO signal that additionally assists for the interpretation and analysis. In case of an isothermal step at 252 °C (Fig. 2 c/d) the first peaks have symmetric shapes and are marked with a green box. If the isothermal step is placed below 252 °C the decomposition is incomplete, which results in an interception and ongoing decomposition when the temperature is further increased. The consequence is the emergence of asymmetric peak shapes of the first and second arising peaks as seen in Fig. 2 a/b (red boxes), where the isothermal step was intentionally set below 252 °C. When the temperature of the isothermal step is above 252 °C, shoulders arise in the ion currents (red bar Fig. 2 e/f) due to the decomposition of the functional group with next-higher thermal stability. Comparison of peak shapes with different isothermal steps confirms that the thermal decomposition of carboxylic groups is concluded at 252 °C. The labeled arrows in the CO^+ ion currents of Fig. 2 refer to the signals caused by the decomposition of different functional groups according to the numbers in Fig. 2. They illustrate, that an isothermal step at too-low temperature leads to a splitting of the decomposition of one functional group and an isothermal step at too-high temperatures impedes thermal separation.

CO_2 is generated from carboxylic, lactone (arm-chair, zig-zag), and anhydrate groups. CO is released by anhydride, phenol, ether and carbonyl groups (Fig. 3c). The optimization of each isothermal step on the basis of the CO_2^+ and CO^+ ion currents is shown in the supporting information.

The decomposition temperature of lactone groups under the release of CO_2 depends on their structural connectivity. When they are located on zig-zag edges they exhibit lower stabilities in comparison to lactones located on arm-chair sites due to different strain of the rings as known from literature [23]. This difference could be confirmed by the thermal separation method, and additionally the corresponding unknown decomposition temperatures, could be determined. Lactones at zig-zag edges decompose between 252 °C and 315 °C whereas lactones at arm-chaired structures show a specific decomposition temperature range between 510 °C and 620 °C.

A special case among the functional groups is the anhydrides, due to the fact that they decompose in two subsequent steps under the release of equimolar amounts of first CO_2 followed by CO. The release of CO_2 between 315 °C and 510 °C is accompanied by the formation of a thermodynamically more stable intermediate that decomposes under the release of CO until 620 °C (Fig. 3a/b). A total decomposition of anhydrates is, therefore, only achieved at 620 °C.

Separation of the phenol and ether functional groups is impossible as their decomposition temperatures overlap. With an isothermal step at 800 °C they could be separated from the decomposition of carbonyls. The step at 1000 °C is the highest technically feasible temperature, a complete decomposition of the carbonyl group is therefore not guaranteed additionally high temperature stable phenol groups as described by Pan and Yang can also not be detected [31].

The ion current profiles of the optimized thermal separation procedure and the schematically visualized decomposition products and windows are shown in Fig. 3 a/b. Fig. 3c visualizes the decomposition temperatures up to the isothermal steps corresponding to the different functional groups of the optimized isothermal TPD analysis. The normed CO^+ and CO_2^+ ion current profiles of nitrosulfuric acid functionalized MWCNT (orange) and graphite (blue) as well as untreated activated char (green) and Vulcan XC75C (red) with the six optimized isothermal steps are displayed. In principle, functional groups that decompose under the release of CO_2 exhibit lower thermal stabilities than functional groups that decompose under the release of CO. As a result of the fifteen times higher surface area of MWCNT compared to graphite, more functional groups could be formed during the functionalization process. This results in a decreasing signal to noise ratio in case of the graphite CO^+ ion current, since the same total masses were used for both samples. However, the CO_2^+ and CO^+ ion current shapes of both materials are comparable after the implementation of the isothermal steps. The analysis of as received active char shows a different quantitative functional group distribution compared to the MWCNT and graphite samples. Active char exhibits a major fraction of higher stable functional groups of phenol/ether and carbonyl groups whereas carboxylic and zig-zag lactone groups are present in a minor scale. Anhydrides and arm-chaired lactones are also visible, but only in a minor extent as seen by the TG data (supporting information S7). Condensation reactions of adjacent carboxylic groups on the active char surface and the formation of anhydrites cannot be confirmed due to only minor water release during the measurement (supporting information S8). The thermal analysis of Vulcan XC75R exhibits that there are only a few functional groups present on the surface. TG data show a mass loss of only 0.2% apart from the loss of physisorbed water (supporting information S7). The CO^+ ion current shows no peaks, small peaks can be observed for the CO_2^+ ion currents. The analysis of different graphitic carbon materials confirm, that the decomposition temperatures depend solely on the thermal stability of the functional groups and are not dependent on the carbon backbone, whereby the developed isothermal TPD analysis is applicable for different carbon materials with graphitic character. Nevertheless, it is noticeable that there is no baseline peak separation of the CO_2^+ and CO^+ ion current of the MWCNT samples at temperatures over 620 °C. It is suggested that gas diffusion as well as adsorption and desorption processes affect the peak width of the desorbed gases in MWCNT samples.

3.2. Comparison of linear and non-linear heating procedure

To determine the benefits and limitations of the linear and isothermal TPD methods, measurements from both heating procedures were compared. The analysis was performed in pure Argon

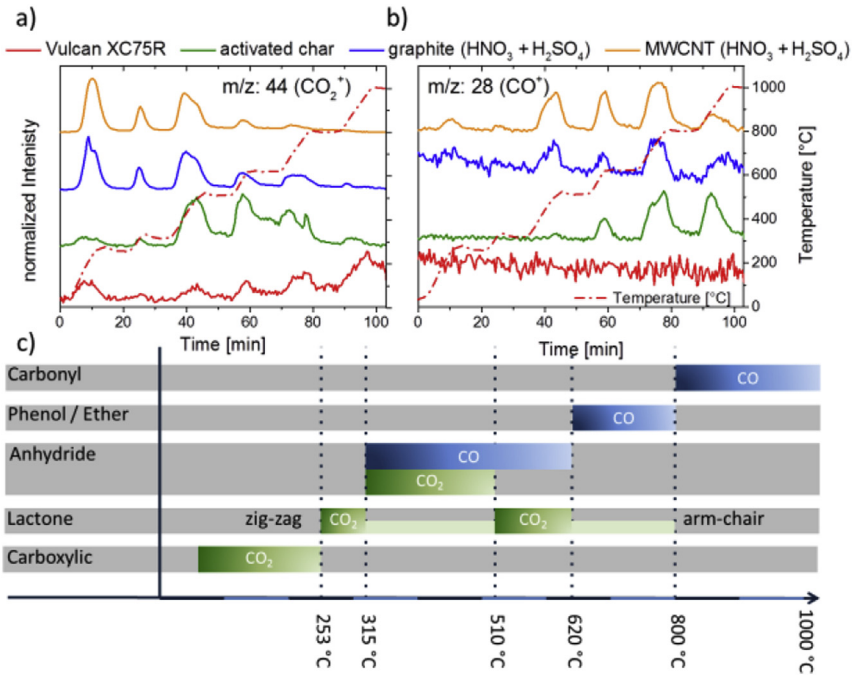

Fig. 3. Isothermal TPD analysis of functionalized MWCNT (orange), graphite (blue), active char (green) and Vulcan X75R (red) to separate different functional groups. The ion currents of *m/z* 44 for CO_2^+ (a) and *m/z* 28 for CO^+ (b) are normalized to 1 for the highest peak and depicted in a stacked way for better comparison. (c) The lower scheme illustrates the temperature ranges of the decomposition of functional groups in combination with the released gaseous products. (A colour version of this figure can be viewed online.)

as well in hydrogen-containing atmosphere (5% H_2 in Ar).The resulting ion current profiles for CO_2^+, CO^+ and H_2O^+ (*m/z* 18) are displayed in Fig. 4.

The CO^+ ion current profiles in Argon and hydrogen-containing atmosphere, recorded with a linear heating rate (Fig. 4b), exhibit significant differences. The most pronounced difference is marked with a yellow box where lower signal intensities are measured in the case of hydrogen containing atmosphere. The peak positions seem to be shifted to lower temperatures as well. The same trend can be observed in the CO_2^+ ion currents profiles (Fig. 4a). The lower thermal decomposition temperatures might due to the a dependence of decomposition mechanism on the atmosphere present, as

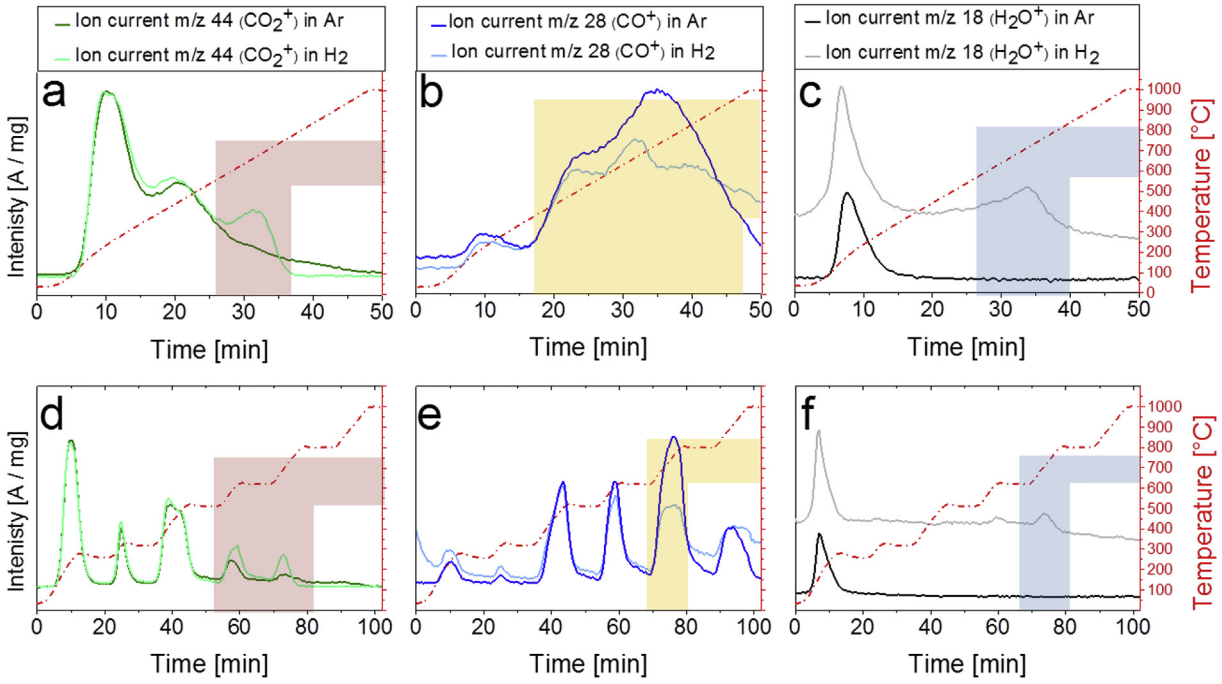

Fig. 4. TG-MS analysis of nitrosulfuric acid functionalized MWCNT in pure argon and 5% hydrogen atmosphere with a linear temperature program (top) and isothermal heating (bottom). The ion currents of (a/d) *m/z* 44 for CO_2^+ (b/e) *m/z* 28 for CO^+ and (c/f) *m/z* 18 for H_2O^+ are shown. Red dashed lines visualize the temperature profiles during the experiment. The colored areas mark the main differences between the measurements in different atmospheres. (A colour version of this figure can be viewed online.)

is known from the literature [32]. Furthermore an additional peak is observed between 600 °C and 750 °C. At the same temperature range, a water signal can be recorded in hydrogen containing atmosphere, which is absent during the measurement in inert gas atmosphere (Fig. 4c). The additional water peak at higher temperatures (blue box) is assumed to be caused by phenol groups, which release water during the decomposition [26]. It cannot be differentiated between in-situ formed phenols and phenol groups that were generated during the acid functionalization procedure.

The corresponding ion current profiles, determined with the isothermal heating program, are shown in the bottom graphs of Fig. 4. The CO signal in hydrogen atmosphere shows a pronounced difference in intensity for the phenol/ether group in comparison to the measurement in pure Argon (Fig. 4e). In inert gas atmosphere, OH species decompose in CO. In the presence of hydrogen, a concurrent reaction of the phenol group decomposition takes place with the formation of water. Therefore, less CO is generated during the thermal analysis in hydrogen atmosphere in step 5. In the case of isothermal heating procedure, the diminished CO intensities (yellow box, step 5) can be directly related to the absence of decomposing CO of the phenol groups, as other signal intensities are not influenced except of a slightly lower peak intensity of step 4. This might arise from the different decomposition temperature and the resulting lower thermal stability of phenol groups in hydrogen atmosphere, as discussed already for the linear heating range.

Regarding the baseline of the CO^+ ion current in both atmospheres, differences can be explained as well by changed decomposition temperatures in dependence of the atmosphere. Functional groups that decompose above 1000 °C in argon atmosphere, fall apart earlier in hydrogen atmosphere and cause the raised baseline [21]. The isothermal steps were optimized for the case of argon atmosphere. This becomes even more pronounced regarding the CO_2^+ signals recorded in argon and hydrogen containing atmosphere (Fig. 4d). The ion current profiles in inert gas atmosphere show symmetric peak shapes, whereas the corresponding signals of the hydrogen atmosphere measurements reveal minor asymmetries. Analogous to the linear heating TPD, increased signal intensities can be obtained in hydrogen containing atmosphere. Furthermore, water can be detected in the same temperature range, where OH decomposes in the case of hydrogen-containing atmosphere. The *m*/*z* 18 signals cannot be detected in pure argon atmosphere (Fig. 4, blue box). The water signal at lower temperature is again an effect of a condensation reaction and removal of adsorbed water.

In general the isothermal TPD procedure allows a much more detailed analysis of the ion currents due to the direct correlation to specific functional groups.

3.3. Validation of thermal separation

Thermal separation will be validated by the application of a selective gas phase deposition technique, namely atomic layer deposition (ALD). Hereby, the metal-containing precursor reacts with specific functional groups of the support material resulting in the formation of a covalent bond. Further detailed information about the ALD process can be found in literature [33]. In the present work vanadium(V) isopropoxide was used as a precursor in combination with water as a co-reactant to deposit vanadium oxides on functionalized MWCNT. The detailed synthesis and characterization of these catalyst materials are reported elsewhere [33,34]. We show here that the precursor reacts selectively with specific functional groups (Fig. 5), and the reaction can be determined by the consumption of the reactive functional groups using the developed isothermal separation process. Therefore linear and isothermal TPD analysis was performed with a V-deposited MWCNT sample

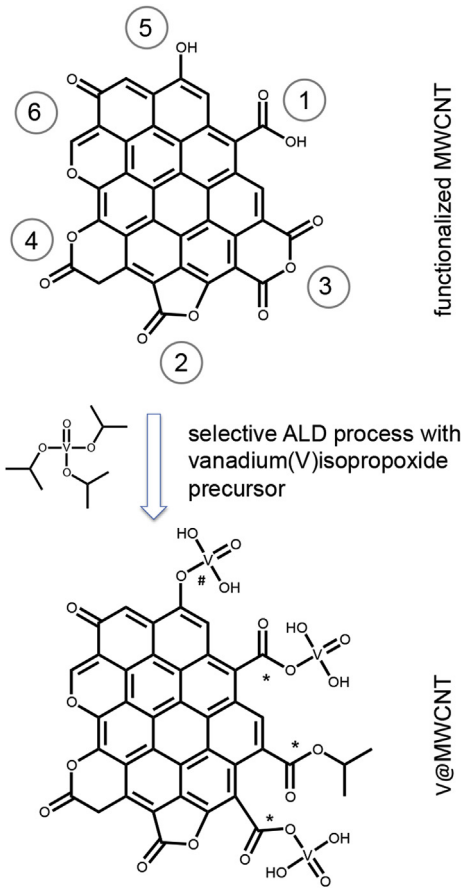

Fig. 5. Selective reactivity of the vanadium(V) isopropoxide precursor in the ALD process with specific functional groups (1,3,5) and the formation of new functional sites (*,#). (A colour version of this figure can be viewed online.)

(V@MWCNT) and compared to the functionalized MWCNT base material without vanadium oxides.

The detected CO^+ and CO_2^+ MS signals of the linear and isothermal temperature program are shown in Fig. 6. The difference spectra illustrate the consumption of functional groups (negative peaks) and indicate an interaction between vanadium oxide and MWCNT (positive peaks) after the ALD process. In the case of the linear heating program (Fig. 6 a/b) a consumption of low thermally stable functional groups can be observed (Fig. 6a). The following temperature range exhibits a higher CO_2 and a lower CO (Fig. 6b) release of the V@MWCNT sample than the functionalized support MWCNT. A distinct correlation to the consumption or formation of new functional groups after the ALD process cannot be assigned.

The difference spectra in Fig. 6 a/b of the isothermal heating program reveal the selective consumption of functional groups after the ALD. The first negative CO_2^+ peak (Fig. 6a) is caused by consumption of carboxylic groups. An uncertain isothermal step would be seen by a consumption of the second peak, but here an increase of the CO_2^+ MS signal is detected confirming the thermal separation of carboxylic groups. Additionally derivatization and therefore consumption of the carboxylic groups was fulfilled with benzoyl chloride (supporting information S9) confirming the thermal separation due to the fact that only the CO_2^+ intensity of the first peak is influenced.

The increased CO_2^+ signal of the difference spectra at step two can be assigned to newly formed, ester-like structures during the ALD process, as marked with an asterisk in Fig. 5. The increased CO_2^+ release is carried out over the whole range of step 2–5 and can be

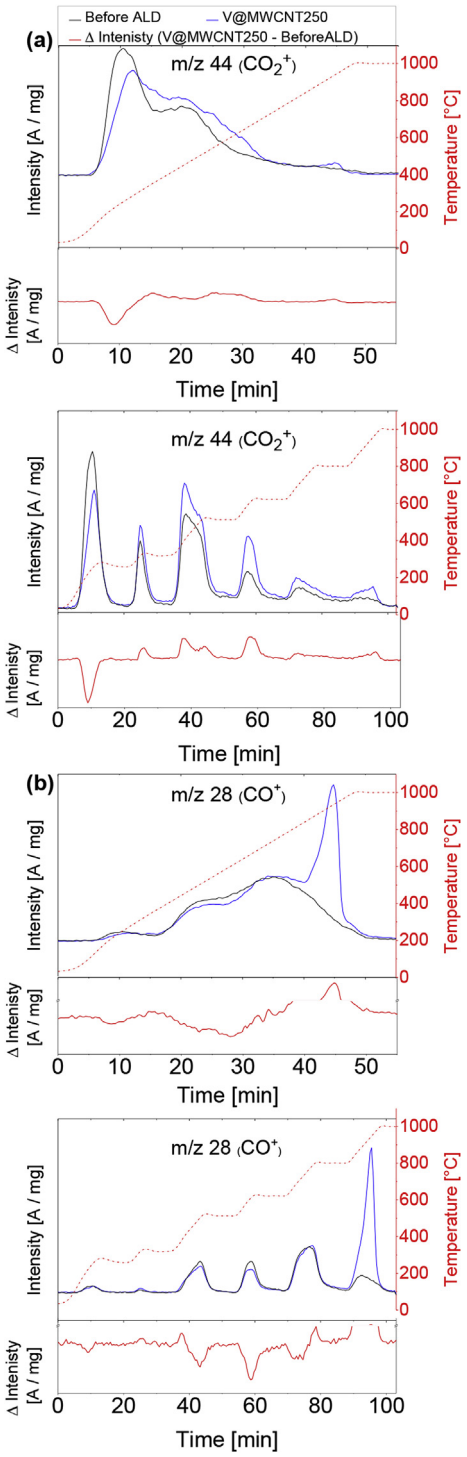

Fig. 6. Comparison of the ion currents of *m*/*z* 28 (CO^+) and *m*/*z* 44 (CO_2^+) during a linear (a) and isothermal (b) TPD analysis before and after the ALD of vanadium oxide. The red dashed line correlates to the applied isothermal temperature profile. (A colour version of this figure can be viewed online.)

caused by ester-like groups with similar thermal stabilities as lactones. Direct interactions between vanadium oxide and MWCNT are also possible. The increased CO_2 release has to be further investigated in detail. A crucial factor here is that during the isothermal step 2, up to 315 °C no CO release can be detected. This observation confirms that subsequent decomposition of the anhydrate group did not take place due to thermal separation during the isothermal step.

The third isothermal step of CO_2^+ and CO^+ MS signal and the fourth isothermal steps of the CO^+ MS signal are attributed to anhydrates. After the deposition of vanadium oxide, a reduced CO^+ signal is detected. This appearance can be explained as well by the formed ester-like structures of the anhydrate group with the precursor. Whereas one part of the precursor forms a O=C-O-$V(O(OH)_2)$ ester-like structure with the anhydrate group, the organic isopropyl part reacts with the appearing intermediate of the anhydrate group, forming again an ester-like structure O=C-O-V (Fig. 5). Both formed structures decompose with release of CO_2, in contrast to the pure anhydrate group, where first CO_2 is released and the formed intermediate decomposes to release CO.

The thermal separation of step 5 from step 6 was already confirmed by the experiments performed in hydrogen containing atmosphere (Fig. 5). The arising water signal, observed at step 5 due to decomposition of phenol groups, cannot be detected at step 6. The drastic increase of the CO^+ signal at step 6 is explained by the reduction of the vanadium species on the MWCNT. The reduction of vanadium was confirmed by XPS measurements, showing a reduced V oxidation state of the ex-situ annealed samples at 1000 °C in comparison to the annealed sample at 800 °C (Fig. S10).

Quantifying the reduction of carboxyl and anhydride groups after the ALD process exhibits a total consumption of 0.3 mmol/g. The amount of deposited vanadium oxide detected via AAS shows a loading of 0.4 mmol/g on the MWCNT surface. Considering that only the consumption of carboxyl and anhydride groups can be taken into account, since the reduction of ALD active phenol groups cannot be analyzed, due to overlaying interactions between carbon and vanadium oxide in the temperature range of phenol group decomposition, the correlation between total consumption of functional groups and the amount of deposited vanadium oxide is clearly visible.

The isothermal temperature program was also applied during the TPD analysis of differently pre-treated MWCNT (Fig. 7). The influence of different acid treatment methods on the formation of oxygen-containing functional groups was investigated.

MWCNT treated with nitrosulfuric acid exhibit the highest amount of (and every kind of) oxygen functional group on their surfaces. Nitric acid treated MWCNT also exhibit every kinds of functional group, but in a lower quantity. Other treatment methods applied to the MWCNT exhibit only minor effects on the formation of functional groups compared to the untreated MWCNT. This finding is in very good agreement with previous studies, where the defect formation of differently treated MWCNT was investigated by Raman spectroscopy [27]. It is notable that after the nitric acid treatment, phenol/ether and arm-chaired lactone groups are more dominant compared to the other functional groups, whereas, after nitrosulfuric acid treatment, the carboxylic, anhydride groups and phenol are very dominant (Fig. 7). The quantitative analysis of anhydride groups via CO_2^+ and CO^+ illustrates again the high quality of peak separation. Anhydrides decompose during the thermal treatment into equal amounts of CO_2 and CO, which could be detected by applying the investigated isothermal step TPD and quantitative analysis of both products. Furthermore, the comparison between pure MWCNT and hydrochloric and sulfuric acid-treated samples exhibit decreasing mass loss caused by the removed amorphous carbon from the surface (TG data supporting information S12). Hydrogen peroxide-treated samples exhibit a slightly increasing CO^+ ion current between 800 °C and 1000 °C, which results from an increase of carbonyl (Fig. 7).

4. Conclusion

In this work, an isothermal step TPD analysis was investigated

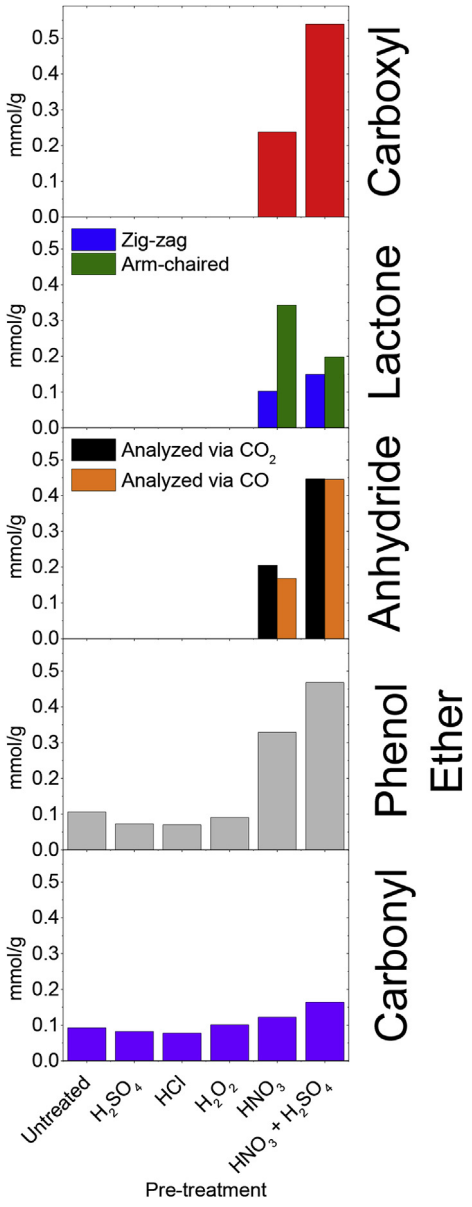

Fig. 7. Isothermal TPD analysis of different pre-treated MWCNT to investigate the influence of the pre-treatment method on the formation of functional groups on the MWCNT surface. The ion currents of m/z 44 CO_2^+ (top) and m/z 28 CO^+ (bottom) are visualized. (A colour version of this figure can be viewed online.)

and compared with linear TPD analysis. The isothermal procedure was used to separate functional groups with different decomposition temperatures. The separation was achieved by the implementation of isothermal steps at the end of each decomposition temperature of a given functional group. The temperature of these isothermal steps was optimized until the isolated CO_2^+ and CO^+ ion currents showed symmetrical peak shapes. The separation by the isothermal steps allowed us to attribute a decomposition event to specific functional groups by interpreting of the detected CO^+ and CO_2^+ signals. In general, CO_2-releasing functional groups like carboxyls, lactones and anhydrides decompose at lower temperatures than CO releasing functional groups like phenols, ether and carbonyls. The behavior in hydrogen-containing atmosphere revealed the decomposition of phenol groups and the formation of H_2O. Additionally, different acid-treated MWCNT were analyzed. It could be shown that only nitric and nitrosulfuric acid treatments have a significant influence on the generation of oxygen-containing functional groups. The ratios between the formed functional groups strongly depend on the treatment method and could be revealed by the isothermal TPD method.

The isothermal analysis was also applied to vanadium containing MWCNT samples, synthesized with a selective gas phase atomic layer deposition (ALD) procedure. Hereby the reaction of specific functional groups (carboxyls, anhydrides, phenols) with the vanadium precursor could be identified. The consumption and generation of specific functional groups was discussed in detail. The direct correlation was not possible when the linear thermal analysis was applied.

To conclude, due to the isothermal temperature program, changes of the CO_2^+ and CO^+ ion currents could assigned. It allows a semi-quantitative analysis of the functional groups present on carbon surfaces. A quantification of the different separated functional groups is impossible by thermal analysis due to the dynamics during the annealing process. At high temperatures, reactions between released gases and functional groups or created defect sites influence the amount of detected gases, as well as conversions of functional groups during the heat treatment.

The approach of isothermal TPD analysis is not limited to the analysis of surface functional groups on carbon materials. It may also be used to analyze serval overlapping events during TPD analysis of materials which were traditionally done with linear thermal TPD analysis. However, for these new applications the isothermal steps have to be optimized accordingly.

Acknowledgment

The author would like to thank the Max Planck society for founding.

Appendix A. Supplementary data

Supplementary data related to this article can be found at https://doi.org/10.1016/j.carbon.2018.01.047.

References

[1] D. Tasis, N. Tagmatarchis, A. Bianco, M. Prato, Chemistry of carbon nanotubes, Chem. Rev. 106 (2006) 1105–1136.
[2] V.N. Popov, Carbon nanotubes: properties and application, Mater. Sci. Eng. R Rep. 43 (2004) 61–102.
[3] M.M.J. Treacy, T.W. Ebbesen, J.M. Gibson, Exceptionally high Young's modulus observed for individual carbon nanotubes, Nature 381 (1996) 678–680.
[4] J. Zhang, M. Terrones, C.R. Park, R. Mukherjee, M. Monthioux, Koratkar, et al., Carbon science in 2016: status, challenges and perspectives, A. Carbon 98 (2016) 708–736.
[5] Y. Sun, K. Fu, Y. Lin, W. Huang, Functionalized carbon nanotubes: properties and applications, Acc. Chem. Res. 35 (2002) 1096–1104.
[6] K. Balasubramanian, M. Burghard, Chemically functionalized carbon nanotubes, Small 2 (2005) 180–192.
[7] A. Stein, Z. Wang, M.A. Fierke, Functionalization of porous carbon materials with designed pore architecture, Adv. Mater 21 (2009) 265–293.
[8] F. Qiang, G. Weinberg, S. Dang-sheng, Selective filling of carbon nanotubes with metals by selective washing, N. Carbon Mater. 23 (2008) 17–20.
[9] M.J. Ledoux, R. Vieira, C. Pham-Huu, N. Keller, New catalytic phenomena on nanostructured (fibers and tubes) catalysts, J. Catal. 216 (2003) 333–342.
[10] P. Serp, M. Corrias, P. Kalck, Carbon nanotubes and nanofibers in catalysis, Appl. Catal. Gen. 253 (2003) 337–358.
[11] A. Sanchez-Sanchez, T.A. Centeno, F. Suarez-Garcia, A. Martinez-Alonso, J.M.D. Tascon, The importance of electrode characterization to assess the supercapacitor performance of ordered mesoporous carbons, Microporous Mesoporous Mater. 235 (2016) 1–8.
[12] C. Leon, L.R. Radovic, Influence of oxygen functional-groups on the performance of carbon-supported catalysts, Abstr. Pap. Am. Chem. Soc. 202 (1991), 33–Fuel.
[13] H.P. Boehm, Some aspects of the surface chemistry of carbon blacks and other carbons, Carbon 32 (1994) 759–769.
[14] S. Szymanski, G. S, G. Rychlicki, Catalytic conversion of propan-2-ol on carbon catalysts, Carbon 31 (1993) 247–257.

[15] G. Hotová, V. Slovák, Quantitative TG-MS analysis of evolved gases during the thermal decomposition of carbon containing solids, Thermochim. Acta 632 (2016) 23–28.
[16] G. Hotová, V. Slovák, Determination of the surface oxidation degree of the carbonaceous materials by quantitative TG-MS analysis, Anal. Chem. 89 (2017) 1710–1715.
[17] J.L. Figueiredo, M.F.R. Pereira, The role of surface chemistry in catalysis with carbons, Catal. Today 150 (2010) 2–7.
[18] J.L. Figueiredo, Functionalization of porous carbons for catalytic Applications, J. Mater. Chem. 1 (2013) 9351–9364.
[19] J.L. Figueiredo, M.F.R. Pereira, M.M.A. Freitas, J.J.M. Orfao, Modification of the surface chemistry of activated carbons, Carbon 37 (1999) 1379–1389.
[20] W.L. Peng, Z. Wang, N. Yoshizawa, H. Hatori, T. Hirotsu, K. Miyazawa, Fabrication and characterization of mesoporous carbon nanosheets-1D TiO_2 nanostructures, J. Mater. Sci. 20 (2010) 2424–2431.
[21] K.F. Ortega, R. Arrigo, B. Frank, R. Schlögl, Trunschke, Acid–Base properties of N-Doped carbon nanotubes: a combined temperature-programmed desorption, X-ray Photoelectron spectroscopy, and 2-propanol reaction investigation, Adv. Compos. Mater. 28 (2016) 6626–6839.
[22] Y. Otake, R.G. Jenkins, Characterization of oxygen-containing surface complexes created on a microporous carbon by air and nitric acid treatment, Carbon 31 (1993) 109–121.
[23] Q.-L. Zhuang, T. Kyotani, A. Tomita, DRIFT and TK/TPD analyses of surface oxygen complexes formed during carbon gasification, Energy Fuels 8 (1994) 714–718.
[24] U. Zielke, K.J. Huttinger, W.P. Hoffman, Surface-oxidized carbon fibers: I. Surface structure and chemistry, Carbon 34 (1996) 983–998.
[25] Q.-L. Zhuang, T. Kyotani, A. Tomita, Carbon. The change of TPD pattern of OS-gasified carbon upon air exposure 32 (1994) 539–540.
[26] B. Marchon, J. Carrazza, H. Heinemann, G.A. Somorjai, TPD and XPS studies of O_2, CO_2, and H_2O adsorption on clean polycrystalline graphite, Carbon 26 (1988) 507–514.
[27] P. Düngen, M. Prenzel, C. Van Stappen, N. Pfänder, S. Heumann, R. Schlögl, Investigation of different pre-treated multi-walled carbon nanotubes by Raman spectroscopy, Mater. Sci. Appl. 8 (2017) 628–641.
[28] A. Peigney, Ch Laurent, E. Flahaut, R.R. Bacsa, A. Rousset, Specific surface area of carbon nanotubes and bundles of carbon nanotubes, Carbon 39 (2001) 507–514.
[29] P.J. Hall, J.M. Calo, Secondary interactions upon thermal desorption of surface oxides from coal chars, Energy Fuels 3 (1989) 370–376.
[30] B. Marchon, W.T. Tysoe, J. Carrazza, H. Heinemann, G.A. Somorjai, Reactive and kinetic properties of carbon monoxide and carbon dioxide on a graphite surface, J. Phys. Chem. 92 (1988) 5744–5749.
[31] Z. Pan, P.T. Yang, Strongly bonded oxygen in graphite - detection by high-temperature TPD and characterization, Ind. Eng. Chem. Res. 31 (1992) 2675–2680.
[32] J.-H. Zhou, Z.-J. Sui, J. Zhu, D. Chen, Y.-C. Dai, W.-K. Yuan, Characterization of surface oxygen complexes on carbon nanofibers by TPD, XPS and FT-IR, Carbon 45 (2007) 785–796.
[33] P. Düngen, M. Greiner, K.H. Böhm, X. Huang, A. Auer, R. Schlögl, et al., Atomically dispersed vanadium oxides on multi-walled carbon nanotubes via atomic layer deposition: a multi-parameter optimization, J. Vac. Sci. Technol. 36 (1) (2018) 01A126.
[34] X. Chen, E. Pomerantseva, P. Banerjee, K. Gregorczyk, R. Ghodssi, G. Rubloff, Ozone-based atomic layer deposition of crystalline V2O5 films for high performance electrochemical energy storage, Chem. Mater. 24 (2012) 1255–1261.